TISSUE ENGINEERING: Part A
Volume 20, Numbers 23 and 24, 2014

DOI: 10.1089/ten.tea.2014.0081

In Vitro and *In Vivo* Studies of BMP-2-Loaded PCL–Gelatin–BCP Electrospun Scaffolds

Bo-Ram Kim, BS,[1] Thuy Ba Linh Nguyen, PhD,[1,2] Young-Ki Min, PhD,[2,3] and Byong-Taek Lee, PhD[1,2]

To confirm the effect of recombinant human bone morphogenetic protein-2 (BMP-2) for bone regeneration, BMP-2-loaded polycaprolactone (PCL)–gelatin (Gel)–biphasic calcium phosphate (BCP) fibrous scaffolds were fabricated using the electrospinning method. The electrospinning process to incorporate BCP nanoparticles into the PCL–Gel scaffolds yielded an extracellular matrix-like microstructure that was a hybrid system composed of nano- and micro-sized fibers. BMP-2 was homogeneously loaded on the PCL–Gel–BCP scaffolds for enhanced induction of bone growth. BMP-2 was initially released at high levels, and then showed sustained release behavior for 31 days. Compared with the PCL–Gel–BCP scaffold, the BMP-2-loaded PCL–Gel–BCP scaffold showed improved cell proliferation and cell adhesion behavior. Both scaffold types were implanted in rat skull defects for 4 and 8 weeks to evaluate the biological response under physiological conditions. Remarkable bone regeneration was observed in the BMP-2/PCL–Gel–BCP group. These results suggest that BMP-2-loaded PCL–Gel–BCP scaffolds should be considered for potential bone tissue engineering applications.

Introduction

Large-sized bone injuries and defects are often repaired using alternative materials such as bone substitutes. Scaffolds play a vital role by serving as templates for host cells and supporting the regeneration of bone defects.[1,2] An ideal scaffold should be biocompatible and biodegradable, and function in a similar manner to the extracellular matrix (ECM).[3] Fibrous scaffolds fabricated by electrospinning have been used recently for biomedical applications because they can easily create a three-dimensional porous structure resembling the morphology of natural ECM.[4–6] The microstructure of electrospun scaffolds such as fiber diameter and porosity can be controlled by adjusting solution properties and operating parameters. Due to the large surface area to volume ratio of electrospun scaffolds, cell adhesion, migration, and proliferation improve.[7–9]

Various types of biomaterials such as natural polymers, synthetic polymers, ceramics, and their composites can be applied to the electrospinning process. The combination of natural and synthetic polymers improves mechanical properties as well as biocompatibility. Polycaprolactone (PCL) is a typical hydrophobic biodegradable synthetic polymer that degrades slowly inside the human body. Due to its slow degradation, it has been investigated mainly as long-term implant material for drug release and support of bone formation.[10–12] Gelatin (Gel), which is a natural polymer derived from collagen, has been widely used for biomaterial applications, such as wound dressings, bone and cartilage regeneration, and drug delivery systems,[13–16] because of its excellent biocompatibility and biodegradability. Several studies have investigated PCL–Gel electrospun scaffolds.[17–20] This approach of using a synthetic/natural polymer blend overcomes the drawback of individual synthetic and natural polymers and improves mechanical properties and biocompatibility.

However, a PCL–Gel polymer system alone cannot provide support for an ideal scaffold because it is not an osteoconductive or osteoinductive material.[21] Natural ECM is composed of fibrous collagen organized in a three-dimensional porous network, and hydroxyapatite (HAp) crystals are dispersed within the collagen fibers.[22] In this study, biphasic calcium phosphate (BCP) nanoparticles were dispersed into a PCL–Gel blend matrix to synthesize a bone mimicking ECM. BCP is a biodegradable and osteoconductive ceramic, which consists of HAp and tricalcium phosphate (TCP) phase compositions. It forms tight bonds with host bone tissues and allows osteogenesis. BCP is a more effective ceramic for bone repair and regeneration than pure HAp or pure TCP alone because it controls the scaffold degradation rate.[23,24] Combining polymers with inorganic materials such as BCP particles can improve the bioactivity of electrospun scaffolds and enhance cell attachment, proliferation, and osteoblastic differentiation.[25–27]

Bone regeneration is regulated by various bioactive agents such as growth factors (bone morphogenetic proteins

[1]Department of Regenerative Medicine, College of Medicine, Soonchunhyang University, Cheonan, Republic of Korea.
[2]Institute of Tissue Regeneration, College of Medicine, Soonchunhyang University, Cheonan, Republic of Korea.
[3]Department of Physiology, College of Medicine, Soonchunhyang University, Cheonan, Republic of Korea.

[BMPs], transforming growth factor-β, fibroblast growth factor, platelet-derived growth factor, and insulin-like growth factor), which are important signals in the osteogenic microenvironment.[28,29] Using osteoinductive growth factors to enhance bone reconstruction and formation on this type of scaffold is the most efficient way to perform protein therapy.[30,31] Among the various types of growth factors, BMPs promote differentiation by inducing mesenchymal stem cells to transform into chondrocytes, osteoblasts, cartilage and then the bone formation.[32,33] In this study, recombinant human BMP-2-loaded PCL–Gel–BCP scaffolds were fabricated using a blend electrospinning process to encapsulate BMP-2 directly inside the fibers. We investigated the effects of BMP-2 on cell proliferation and differentiation of MC3T3-E1 cells and focused on osteogenesis in a rat calvarial skull model.

Materials and Methods

Preparation of the BMP-2-loaded PCL–Gel–BCP solution

PCL (Mn 70,000–90,000) and Gel type A (300 Bloom) from porcine skin were purchased from Sigma-Aldrich (St. Louis, MO). 2,2,2-Trifluoroethanol (TFE, purity >99.0%; Alfa Aesar, Cambridge, United Kingdom) was used as the solvent. BCP nanopowder was synthesized by a microwave-assisted process.[34] The concentration and ratio of each solution were prepared according to a method reported previously.[17] To fabricate the electrospun scaffolds, 10% w/v PCL and 10% w/v Gel solutions were prepared by dissolving 1 g of each polymer in TFE separately followed by stirring overnight at room temperature. The 10% w/v Gel solution was added to the 10% w/v PCL solution until it was mixed completely at a volume 50:50 ratio of PCL:Gel. BCP particles (size, 45–50 μm) were dispersed in TFE by ultrasound and added to the PCL–Gel solution at a ratio of BCP: PCL:Gel = 1:1:1 (w/w) and stirred for 2 h to make the scaffold blended BCP. In addition, 0.5 μg/mL recombinant BMP-2 (10 μg, >95% purity; R&D Systems Minneapolis, MN) was mixed with the PCL–Gel–BCP solution before starting the electrospinning process.[35]

Fabrication of the electrospun scaffolds

The PCL–Gel–BCP scaffolds and BMP-2-loaded PCL–Gel–BCP scaffolds were fabricated by an electrospinning process. Five milliliters of the solution was loaded into a 12 mL plastic syringe fitted with an 18-gauge needle and injected using a syringe-pump at a flow rate of 0.5 mL/h. The collector was covered with a piece of aluminum foil. The distance between the tip of the needle and the collector was about 10 cm, and 20 kV voltage was applied.

The fabricated electrospun scaffolds were cross-linked using 1-ethyl-3 (3-dimethylaminopropyl) carbodiimide (EDAC) and *N*-hydroxysuccinimide (Sigma-Aldrich) at a 5:2 molar ratio in 80% ethanol for 1 h at 4°C, rinsed three times with distilled water for 5 min to remove residual EDAC, frozen at −20°C for 4 h, and then freeze-dried at −80°C.

Scaffold characterization

Morphological analysis. The surfaces of the PCL–Gel–BCP and BMP-2/PCL–Gel–BCP scaffolds were sputter-coated with platinum (Cressington 108 Auto, Cambridge, United Kingdom) and observed by scanning electron microscopy (SEM, JSM-6701F; Jeol, Tokyo, Japan) at an accelerating voltage of 10 kV. The average fiber diameter of the electrospun fibers was measured from the SEM images. At least 10 positions on the fiber mat were tested to measure the electrospun fiber diameter. The energy dispersive X-ray spectrometer (EDS, JSM-7401F) was used to analyze the elemental composition of the electrospun fibers. The elemental composition of the crystal structures and the composition of the scaffolds were analyzed by X-ray diffraction (XRD, D/MAX-2500V; Rigaku, The Woodlands, TX). The diffraction angle was varied from 10° to 60° 2θ.

BMP-2 release study. To determine whether BMP-2 loaded successfully, BMP-2-loaded PCL–Gel–BCP scaffolds were observed by immunofluorescent staining and compared with PCL–Gel–BCP scaffolds (negative control). The scaffolds were washed with phosphate-buffered saline (PBS) and treated with 5% bovine serum albumin (BSA) for 30 min. The scaffolds were blocked with BMP-2 primary antibody (BMP-2/4 [H-1], 1:50; Santa Cruz Biotechnology, Santa Cruz, CA) for 4 h and rinsed with PBS three times. BMP-2 secondary antibody (goat anti-mouse IgG-FITC; Santa Cruz Biotechnology) (1:100) was applied for 1 h and washed again with PBS. After staining, confocal microscopy (FV10i-W) was performed to measure BMP-2 loading on the scaffolds.

The *in vitro* release rate of BMP-2 from the PCL–Gel–BCP scaffolds was measured with a BMP-2 enzyme-linked immunosorbent assay (ELISA) kit (R&D Systems). To collect the supernatant, the BMP-2-loaded PCL–Gel–BCP scaffolds were immersed in 1 mL PBS and incubated at 37°C. At various times, all of the supernatant was collected, and replaced with fresh PBS. The amount of BMP-2 in the supernatants was determined according to the manufacturer's protocol. Absorbance was read with an ELISA reader (Infinite F50; Tecan, Zurich, Switzerland) at a wavelength of 450 nm.

In vitro *study*

Cell culture. Preosteoblast MC3T3-E1 cells, derived from mice, were cultured in minimum essential medium-alpha (MEM-α; Gibco, Grand Island, NY) supplemented with 10% fetal bovine serum (FBS; Gibco) and 1% penicillin/streptomycin (P/S). The MC3T3-E1 cells were maintained in a humidified incubator at 37°C in a 5% CO_2 atmosphere.

Cell adhesion. Electrospun nanofibers were initially sterilized under UV light, sterilized further with 70% ethanol, washed with PBS, and finally soaked in MEM-α. MC3T3-E1 cells were seeded on 1 cm^2 of scaffolds at a density of 10^4 cells/cm^2 in a 24-well plate with culture medium. To observe cell adhesion, the cells were cultured for 60 and 90 min. After culturing, the cells were fixed in 2% glutaraldehyde (DeaJung Co., Seoul, Korea) and dehydrated in an ethanol series (50%, 70%, 90%, and 100%) (Merck, Darmstadt, Germany). The dehydrated cells were dried in hexamethyldisilazane (DeaJung Co) and observed by SEM. The cells were immunostained using fluorescein isothiocyanate (FITC)-conjugated phalloidin (25 μg/mL; Sigma-Aldrich) and vinculin (Millipore, Billerica, MA) for confocal microscopy.

The cells on the scaffolds were fixed in 4% paraformaldehyde (Sigma-Aldrich) for 10 min at room temperature, permeabilized in 0.25% Triton X-100 (Sigma-Aldrich) for 10 min, and blocked in 2.5% BSA for 1 h. The cells were immunostained using vinculin antibody at 4°C overnight. After washing with PBS, the cells were stained with FITC-conjugated phalloidin for 30 min. Nuclei were stained with Hoechst. Finally, the scaffolds were mounted on glass slides and visualized under a confocal fluorescent microscope (FV10i-W) using the accompanying FV10i-ASW 3.0 viewer software.

Cell viability. To evaluate cell proliferation, the PCL–Gel–BCP and BMP-2/PCL–Gel–BCP scaffolds were analyzed using the 3-[4,5-dimethyl-2-thiazolyl]-2,5-diphenyltetrazolium bromide (MTT) assay (Sigma-Aldrich).[36] After 1, 3, and 7 days of culture, 100 μL of MTT solution was added to each well filled with PCL–Gel–BCP and BMP-2/PCL–Gel–BCP scaffolds and incubated for 4 h. After removing the media, 1 mL dimethyl sulfoxide (Samchun Pure Chemical Co., Seoul, Korea) was added to each well to extract the formazan crystals under gentle shaking. The extract of each scaffold was transferred to a 96-well plate and the absorbance intensities were measured at 595 nm using an ELISA reader.

Cell proliferation and attachment. Confocal microscopy was performed to observe growth of MC3T3-E1 cells (1×10^4 cells/well) seeded on the PCL–Gel–BCP and BMP-2/PCL–Gel–BCP scaffolds. Briefly, after 1, 3, and 7 days of culture, the scaffolds were rinsed with PBS twice and fixed in 4% paraformaldehyde for 10 min at room temperature, permeabilized in 0.25% Triton X-100 for 10 min, and blocked in 2.5% BSA for 1 h. The cells were immunostained using FITC-conjugated phalloidin overnight at 4°C. Nuclei were stained with Hoechst. Cell behavior was observed under a confocal microscope at 10× and 60× magnifications.

Cell differentiation. The osteogenic differentiation of MC3T3-E1 cells was analyzed using immunocytochemical analysis of alkaline phosphate (ALP) and osteopontin (OPN). MC3T3-E1 cells were cultured on PCL–Gel–BCP and BMP-2/PCL–Gel–BCP scaffolds using osteogenic medium consisting of MEM supplemented with 10% FBS, 1% P/S, 10 nM dexamethasone (Sigma-Aldrich), 50 μg/mL L-ascorbic acid (Sigma-Aldrich), and 10 mM β-glycerophosphate disodium salt hydrate (Sigma-Aldrich). After 7 and 14 days, cells on the scaffolds were stained with rabbit ALP antibody (1:50; Santa Cruz Biotechnology) and mouse OPN antibody (1:50; Santa Cruz Biotechnology) overnight at 4°C. Then, the scaffolds were incubated in secondary antibody (Alexa Fluor 488, 1:1000; Invitrogen, Carlsbad, CA). The images were visualized under a confocal microscope using 60× magnification.

In vivo *study*

Implantation of the BMP-2/PCL–Gel–BCP scaffolds in the rat skull. A total of 16 male Sprague–Dawley rats, weighing 300 g, were used for the *in vivo* study of PCL–Gel–BCP and BMP-2/PCL–Gel–BCP scaffolds (four rats each), after the protocol was approved by the Animal Ethics Committee of the Soonchunhyang University. The healing process was observed 4 and 8 weeks after implantation. The PCL–Gel–BCP and BMP-2/PCL–Gel–BCP scaffolds were sterilized with 70% ethanol, washed with PBS, and finally freeze-dried at −80°C for 3 h before use. The rats were anesthetized with diethyl ether, and the hair on the skull was shaved and sterilized with 70% ethanol and povidone iodine. After exposure of the parietal skull, two defects were made on the left and right side of the skull (5 mm diameter, and 1 mm thickness) using a trephine drill. One defect was grafted with PCL–Gel–BCP scaffold and the other defect was sutured without a sample as a negative control. The BMP-2/PCL–Gel–BCP scaffolds were implanted in the same way. The subcutaneous tissue was closed and the skin was resutured. The rats were sacrificed 4 and 8 weeks after implantation.

Micro-computed tomography and histological analysis. Four and 8 weeks after implantation, the rats were sacrificed and the entire portion of the defective skull was removed. The samples were fixed in 10% formalin solution at room temperature. Micro-computed tomography (Micro-CT) (Skyscan 1076, Antwerp, Belguim) was performed to observe new bone formation at the defect sites. Each sample was fixed on the object stage, and imaging was performed on the sample for 360° of rotation with an exposure rate of 20 min per frame. Micro-CT images were reconstructed using CTAn (Skyscan) and CTVol (Skyscan) to make three-dimensional images. The bone volume (BV) and percent bone volume [bone volume (BV)/tissue volume (TV) (%)] were calculated to evaluate the new bone quantity.

The rat skulls fixed in 10% formalin solution were decalcified using 5% HNO_3. The tissues were embedded in a paraffin block and serially cut using a microtome (HM 325; Thermo Scientific, Rockford, IL). The 4 ± 2 μm thick sections were mounted on microscope slides. The slides were deparaffinized and hydrated with xylene and an alcohol series. The slides were then stained with hematoxylin–eosin (H&E) and Masson's trichrome (M-T). The tissue sections were viewed with an Olympus BX53 microscope and photographed with an Olympus DP72 camera. Images were analyzed using the Cellsens software.

Immunohistochemistry. Immunohistochemical staining of the BMP-2/PCL–Gel–BCP implanted group at 8 weeks was performed using the EnVision™ kit (K5007; Dako, Carpentaria, CA) to determine differentiation simulation *in vivo*. The tissue sections were heated with a citrate buffer for antigen retrieval, blocked with normal blocking serum for 15 min, and then incubated with anti-OPN (1:100; Santa Cruz Biotechnology) and anti-osteocalcin (OCN; 10 μg/mL; Abcam, Cambridge, United Kingdom) for 1 h. After washing, the sections were incubated with the secondary antibody (Envision/HRP) for 30 min and finally were stained with substrate-chromogen solution 3,3′-diaminobenzidine tetrahydrochloride (DAB) and hematoxylin. The tissue sections were viewed and examined using an Olympus BX53 light microscope equipped with the CellSens software.

Statistical analyses

All statistical analyses were performed using the SPSS (Statistical Package for the Social Science, version 16, SPSS, Inc., Chicago, IL). Results are expressed as mean ± standard deviation.[37] Student's *t*-test was used to compare different treatment groups, with significance assigned at $p < 0.05$.[38]

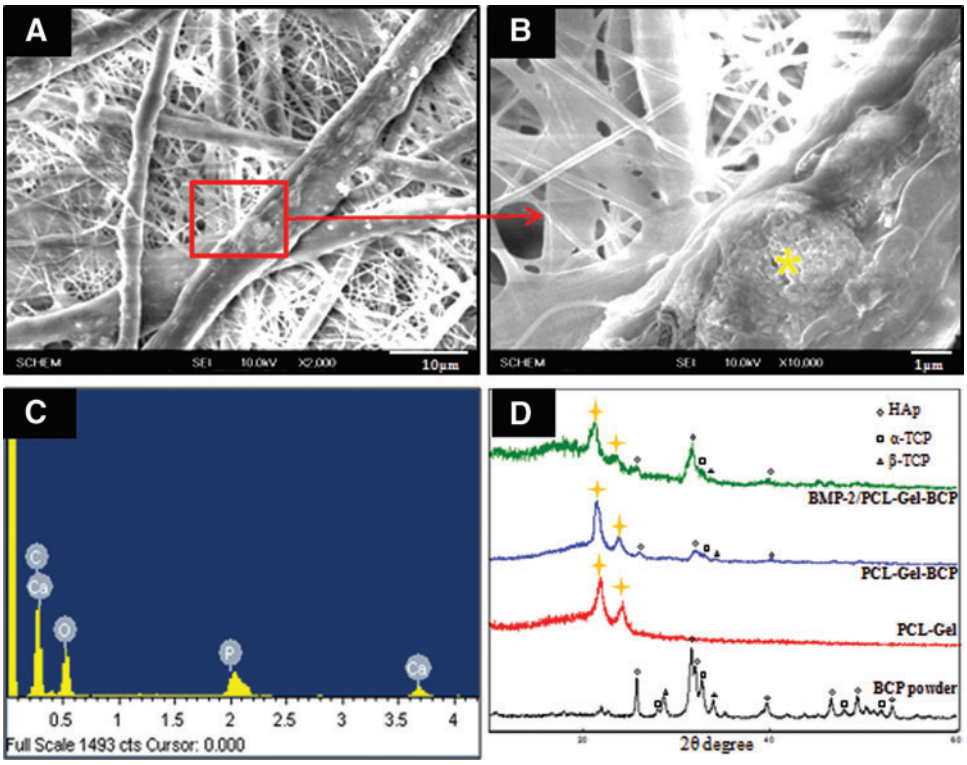

FIG. 1. The morphology evaluated by scanning electron microscope of polycaprolactone (PCL)–gelatin (Gel)–biphasic calcium phosphate (BCP) **(A, B)** electrospun scaffolds and the compositions of these electrospun scaffolds were analyzed by energy dispersive X-ray spectrometer profile **(C)** and X-ray diffraction spectra profiles **(D)**. The yellow asterisk (*) indicates spectrum measured location. Color images available online at www.liebertpub.com/tea

Results

Characterization of the PCL–Gel–BCP and BMP-2/PCL–Gel–BCP scaffolds

Figure 1(A, B) shows the SEM morphology of the randomly arranged fibers generated from the PCL–Gel–BCP scaffolds. The PCL–Gel–BCP scaffolds had a well connected fibrous structure composed of various diameters from nano-sized to micro-sized fibers (100 nm–10 μm). The average diameter of the fibers is shown in Table 1. BCP nanoparticles were deposited on the scaffold surface, and they affected the surface topography. The surface morphology of the BCP loaded PCL–Gel fiber was rough. The EDS spectrum in Figure 1(C) revealed a high concentration of Ca and P at a Ca/P ratio of 1.64. It is concluded that the BCP nanoparticles were distributed well in the PCL–Gel fibers. XRD measurements were performed to examine whether the BCP particles were blended successfully with the PCL–Gel solution. The XRD pattern of the PCL–Gel–BCP electrospun scaffolds was similar to the PCL–Gel scaffold curve and contained specific strong peaks at ~21–22° and 23–24° (2θ), as indicated by the marks [Fig. 1(D)]. The pattern also had specific peaks, which are the characteristic pattern of a BCP particle curve, but some peaks did not appear at 28–29°. The disappearance of the peaks showed that the BCP particles were well loaded within the fibers and that they were not only on the surface. Overall, this result confirmed that the BCP particles were well distributed in the PCL–Gel scaffolds and that the ceramic/polymer blends were prepared successfully. However, no significant change in the crystalline character was observed in the BMP-2/PCL–Gel–BCP compared with that of the PCL–Gel–BCP scaffolds.

Fluorescent staining was performed using the BMP-2 antibody to confirm BMP-2 loading on the PCL–Gel–BCP scaffolds. As shown in Figure 2(A), confocal imaging demonstrated that the BMP-2-loaded PCL–Gel–BCP scaffolds exhibited strong positive staining compared with that of the PCL–Gel–BCP only scaffolds [Fig. 2(B)]. This result shows that BMP-2 was distributed properly on the scaffolds. In addition, the BMP-2 release rate from the scaffolds was measured by quantitative ELISA [Fig. 2(C)]. After 24 h, the cumulative release from 0.5 μg/mL BMP-2-loaded PCL–Gel–BCP scaffolds was 32.1% ± 5.83% of the original amount and increased up to 54.4% ± 9.22% after 7 days. Burst release occurred during the first few days because some BMP-2 molecules existed on the outside of the fibers where they could easily diffuse out without fiber biodegradation. After burst release, the BMP-2 release behavior was sustained. According to when polymer degradation started, the remaining BMP-2 that was present on the inside of the fibers was released slowly. The total released BMP-2 after 31 days was 83.16% ± 11.33% compared with that of the initial concentration.

In vitro *studies*

Cell attachment and proliferation on electrospun scaffolds. Electrospun scaffolds provide an environment similar

TABLE 1. AVERAGE FIBER DIAMETER OF PCL–GEL–BCP AND BMP-2/PCL–GEL–BCP

Samples	*Average diameter of fibers*[a] *(μm)*
PCL–Gel–BCP	3.0 ± 0.5
BMP-2/PCL–Gel–BCP	3.0 ± 0.4

[a]All data are expressed as mean ± standard deviation.
BCP, biphasic calcium phosphate; BMP-2, bone morphogenetic protein-2; Gel, gelatin; PCL, polycaprolactone.

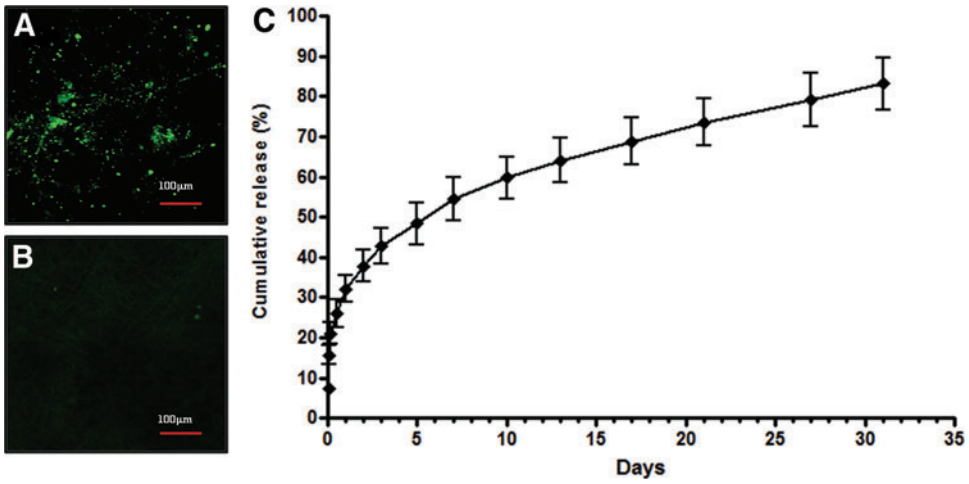

FIG. 2. Immunofluorescent staining to confirm bone morphogenetic protein-2 (BMP-2) identification [with BMP-2 **(A)**, and without BMP-2 **(B)** on the PCL–Gel–BCP scaffolds] and BMP-2 release rate graph **(C)**. Color images available online at www.liebertpub.com/tea

to the ECM for cell adhesion, migration, and proliferation. The degree of adhesion and proliferation of host cells on the material indicates the biocompatibility of that material. To confirm biocompatibility, MC3T3-E1 cells were cultured on the PCL–Gel–BCP and BMP-2/PCL–Gel–BCP scaffolds. Figure 3(A) shows the attachment behavior of the MC3T3-E1 cells on the electrospun scaffolds after 60 and 90 min of incubation. The cells were well attached on both scaffolds with and without BMP-2 after 60 min [Fig. 3(A)-a1, a3]. The cells were more spread out in the case of the BMP-2/PCL–Gel–BCP

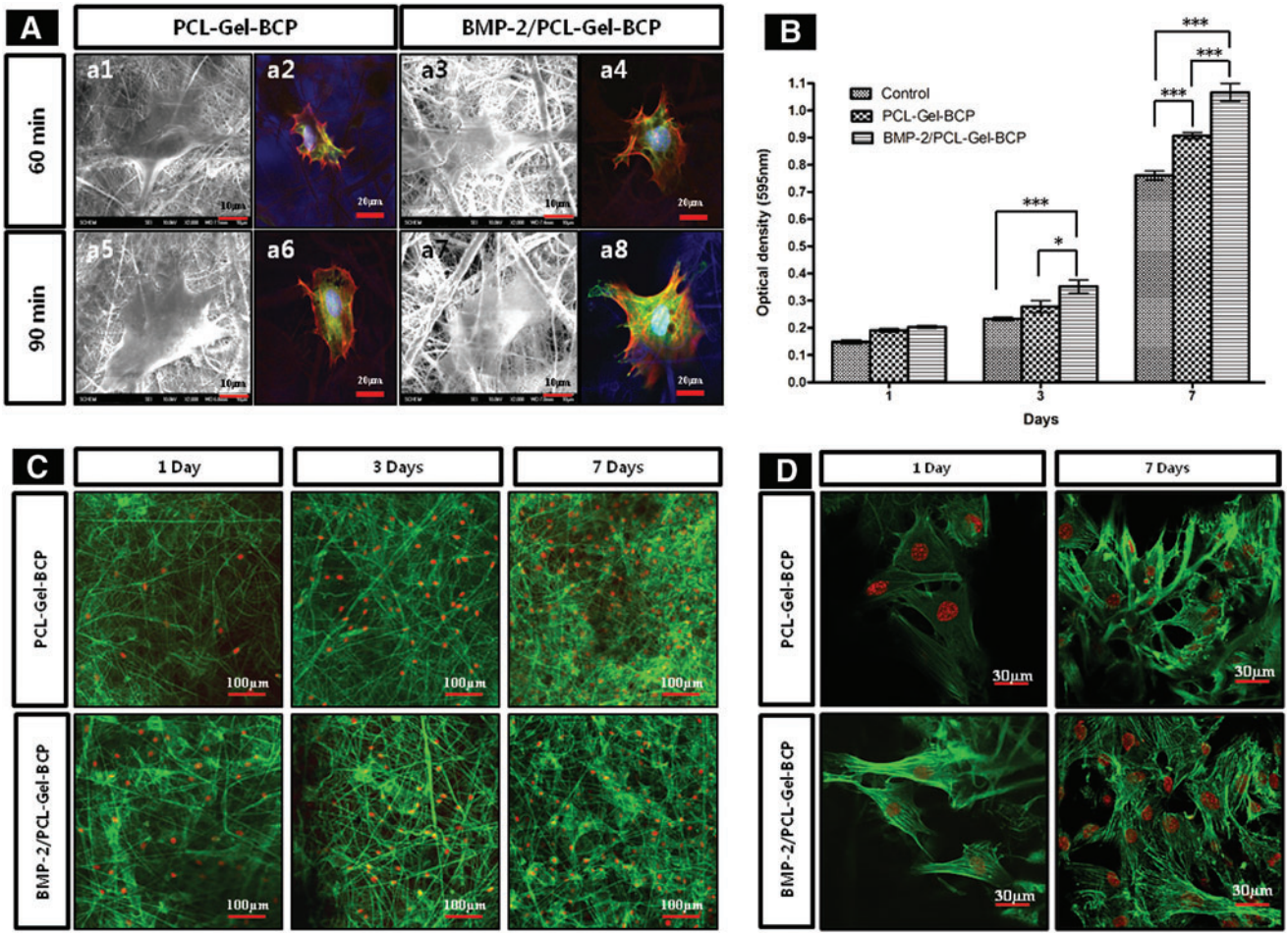

FIG. 3. **(A)** Cell adhesion behaviors on PCL–Gel–BCP and BMP-2/PCL–Gel–BCP scaffolds after seeding (60, 90 min) were observed by scanning electron microscopy **(a1, a3, a5, a7)** and confocal microscope **(a2, a4, a6, a8)**. Vinculin, phalloidin, and nucleus were labeled with green, red, and blue, respectively. MC3T3-E1 cell viability and proliferation on tissue culture plates (control), PCL–Gel–BCP and BMP-2/PCL–Gel–BCP scaffolds were determined by an MTT assay **(B)** and F-actin staining **(C)**. Cell attachment behavior after 1 and 7 days also observed at high magnification (60×) **(D)**. $*p < 0.05$; $***p < 0.001$. Color images available online at www.liebertpub.com/tea

scaffolds, and they passed through the scaffold pores [Fig. 3(A)-a7] compared with that of the PCL–Gel–BCP scaffolds after a 90 min incubation [Fig. 3(A)-a5]. In addition, immunostaining for focal adhesion and the actin cytoskeleton was performed [Fig. 3(A)-a2, a4, a6, a8]. Vinculin, F-actin, and nuclei were detected as green, red, and blue, respectively. Focal adhesion and the cytoskeletal filaments of the cells were more clearly observed on the BMP-2/PCL–Gel–BCP scaffolds than those without BMP-2 [Fig. 3(A)-a8]. These images demonstrate that the BMP-2-loaded scaffolds promoted improved cell attachment and spreading. Cell proliferation on the PCL–Gel–BCP and BMP-2/PCL–Gel–BCP scaffolds as well as the control (tissue culture plate) was evaluated by the MTT assay and immunofluorescence staining after a 1, 3, and 7 days of incubation. As shown in Figure 3(B), the cells continuously proliferated on all samples. After 7 days in culture, the optical density (OD) value was the highest for the BMP-2/PCL–Gel–BCP scaffolds. This trend was also observed in the confocal micrographs [Fig. 3(C)]. In particular, a higher number of cells were attached on the BMP-2/PCL–Gel–BCP scaffolds than on the PCL–Gel–BCP scaffolds in the enlarged images shown in Figure 3(D), and the cells were larger and healthier. This result was well matched with the short incubation time as shown in Figure 3(A). Figure 3(D) shows that the well-developed cytoskeletal structure and dense cellular network were interconnected with the BMP-2/PCL–Gel–BCP scaffolds after 7 days. The MC3T3-E1 cells attached and proliferated well on all samples, and the BMP-2-loaded scaffolds showed better biocompatibility.

Cell differentiation. To investigate the effects of BMP-2 on osteogenic differentiation behavior, MC3T3-E1 cells were cultured on the PCL–Gel–BCP and BMP-2/PCL–Gel–BCP scaffolds under osteogenic medium conditions. Figure 4 shows the expression of ALP and OPN. Both scaffolds expressed ALP and OPN at 7 and 14 days (labeled in green). The BMP-2-loaded scaffolds had more intense ALP activity at the early stage compared with ALP expression at 7 days than those without BMP-2. Furthermore, OPN activity increased at 14 days on the BMP-2/PCL–Gel–BCP scaffolds. Osteogenesis of the cells was triggered at an earlier stage by loading BMP-2 on the PCL–Gel–BCP scaffolds.

In vivo *studies*

Micro-CT analysis. Figure 5(A) shows typical three-dimensionally reconstructed images of PCL–Gel–BCP and BMP-2/PCL–Gel–BCP scaffolds as well as the negative control (defect only) group after 4 and 8 weeks in the rat skull. Bone formation in the BMP-2/PCL–Gel–BCP group was markedly higher at 4 weeks postimplantation, and the center of the defect was filled with new bone, whereas the defect site containing the PCL–Gel–BCP scaffolds and the control group had a small amount of bone that formed

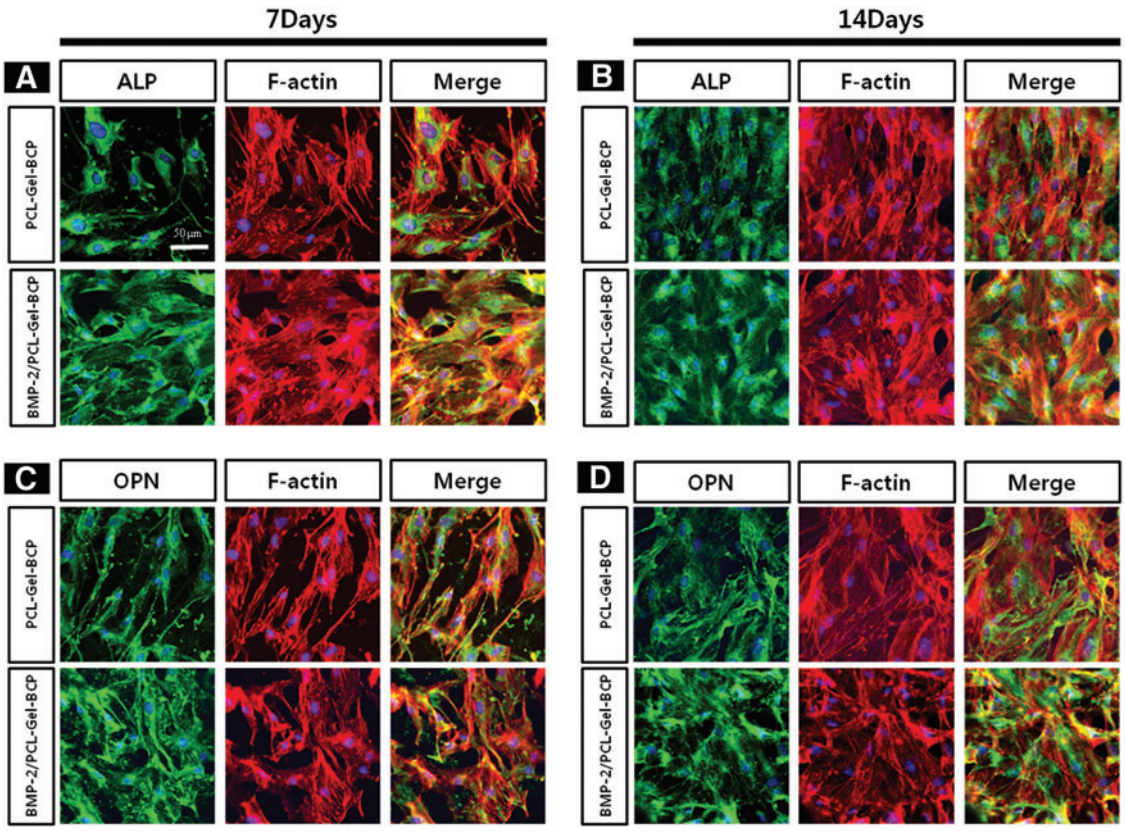

FIG. 4. Exploring the effect of BMP-2 loading on cell differentiation. Immunostaining of MC3T3-E1 cells labeled with alkaline phosphate (ALP) **(A, B)** and osteopontin (OPN) **(C, D)** were observed by confocal microscope at high magnification (60×) after culturing at 7 days **(A, C)** and 14 days **(B, D)**. Color images available online at www.liebertpub.com/tea

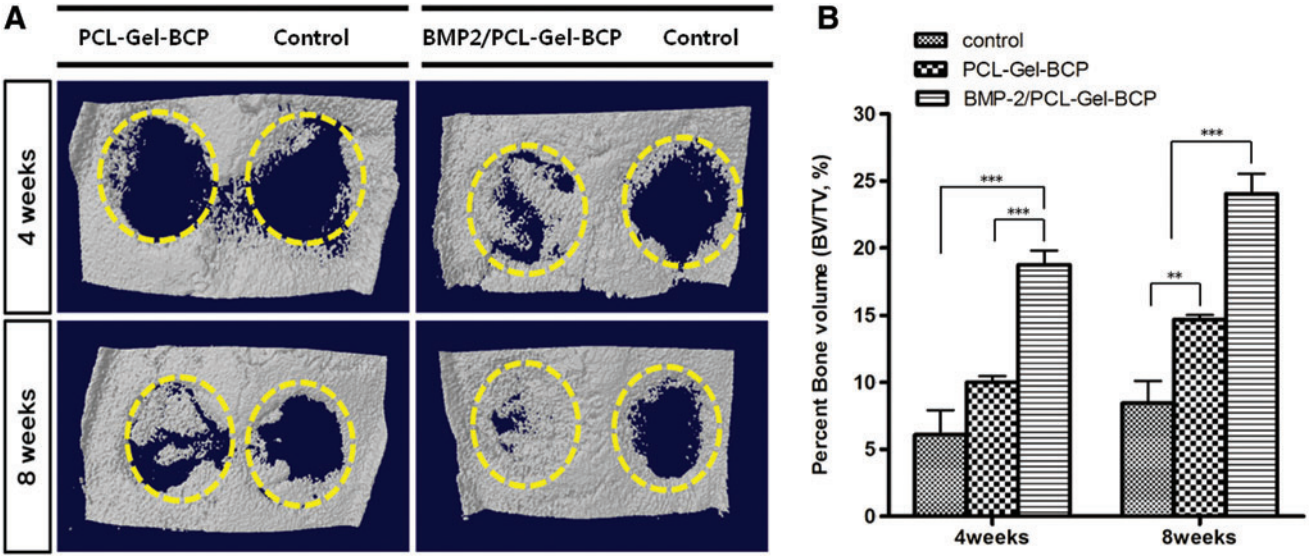

FIG. 5. Reconstructed three-dimensional micro-computed tomography image **(A)** and quantitative analysis of percent bone volume (BV/TV) **(B)** at the defect (negative control), PCL–Gel–BCP and BMP-2/PCL–Gel–BCP scaffolds after 4 and 8 weeks of postimplantation. The dotted circles indicate defect zones. $^{**}p<0.01$; $^{***}p<0.001$. Color images available online at www.liebertpub.com/tea

from the edge of the host bone. In contrast, the defect was almost covered with new bone in the BMP-2/PCL–Gel–BCP group after 8 weeks. Figure 5(B) shows the quantitative analysis of newly formed bone at the defect site. The percent bone volume (BV/TV%) in the BMP-2/PCL–Gel–BCP group (24.05% ± 2.98%) after 8 weeks was greater than that of the PCL–Gel–BCP group (14.7% ± 0.70%) and the control group (8.45% ± 3.34%). This result clearly demonstrates that BMP-2 improved bone formation within a short period.

Histological analysis. A histological evaluation of extracted bone samples from the control, PCL–Gel–BCP, and BMP-2/PCL–Gel–BCP groups was performed after 4 and 8 weeks to confirm new bone formation (Figs. 6 and 7). H&E staining of the tissue sections revealed significantly different amounts of new bone formation in the groups. The defect zone of the control group only had fibrous connective tissue at 4 weeks [Fig. 6(A)]. In contrast, the PCL–Gel–BCP and BMP-2/PCL–Gel–BCP groups revealed newly formed bone and dense connective tissue from the edge of the interface between the scaffolds and the host bone. The result at 8 weeks [Fig. 6(B)] was similar [Fig. 6(A)], and the new bone area had increased significantly. The presence of dense collagen composed of osteoblasts was confirmed by the blue

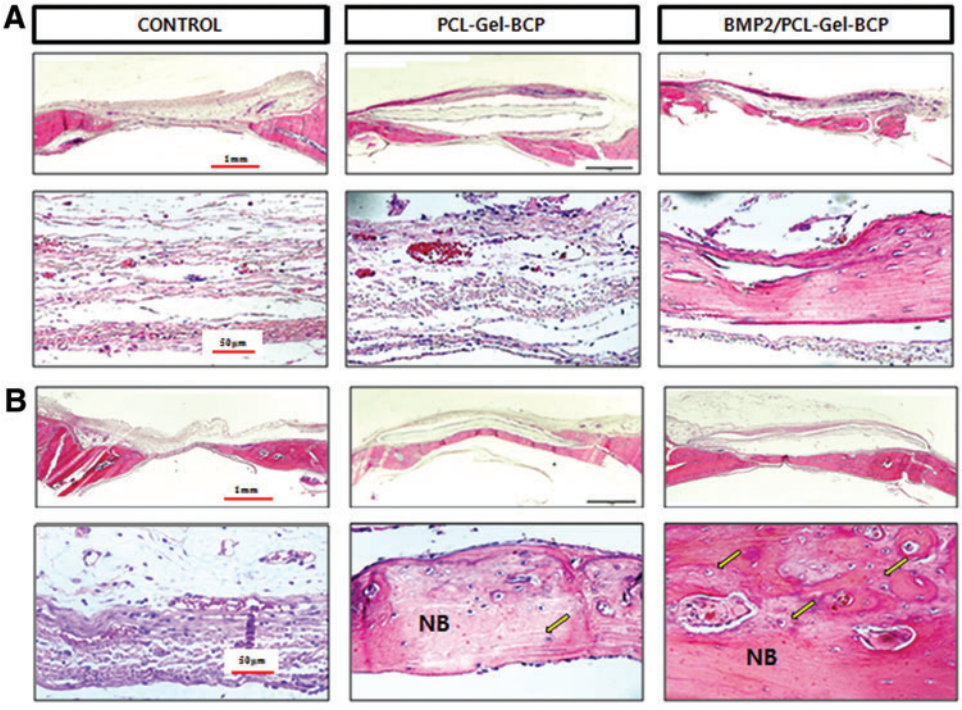

FIG. 6. Histological cross-sections of rat skull with implanted PCL–Gel–BCP and BMP-2/PCL–Gel–BCP scaffolds and negative control (defect only) stained by hematoxylin–eosin method at **(A)** 4 weeks and **(B)** 8 weeks. NB indicates newly formed bone; arrow indicates osteocyte. Color images available online at www.liebertpub.com/tea

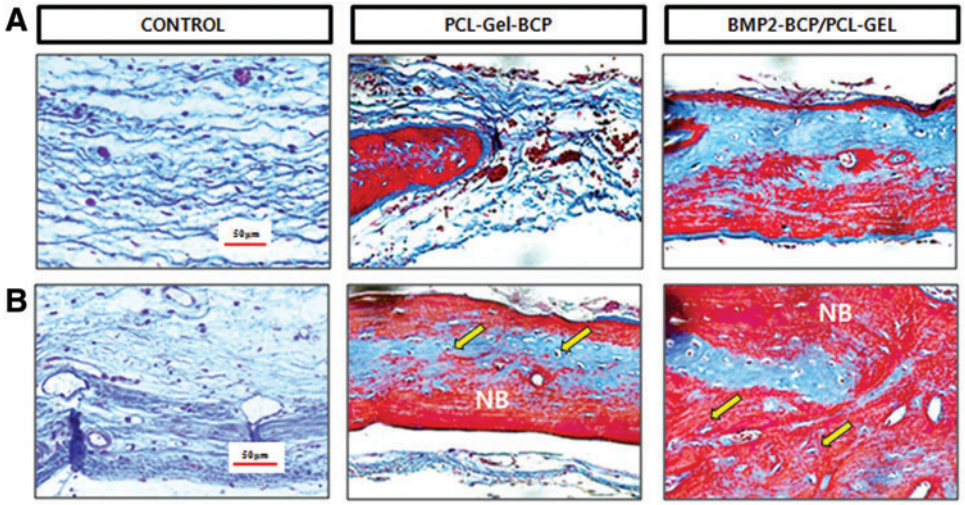

FIG. 7. Histological cross-sections of rat skull with implanted PCL–Gel–BCP and BMP-2/PCL–Gel–BCP scaffolds and negative control (defect only) stained by Masson's trichrome method at **(A)** 4 weeks and **(B)** 8 weeks. NB indicates newly formed bone; arrow indicates osteocyte. Color images available online at www.liebertpub.com/tea

staining of the M-T stained sections, as shown in Figure 7. Significant new bone was formed at the center of BMP-2/PCL–Gel–BCP scaffolds compared with that in the PCL–Gel–BCP and control groups [Fig. 7(A)]. The collagen rich sites had decreased in size and were replaced with new bone [Fig. 7(B)]. Osteoblasts and osteocytes increased in number with the addition of BMP-2 to the scaffolds, and the defect site was perfectly regenerated with new bone.

Immunohistochemical staining was performed in the BMP-2/PCL–Gel–BCP group at 8 weeks. Figure 8(A) shows

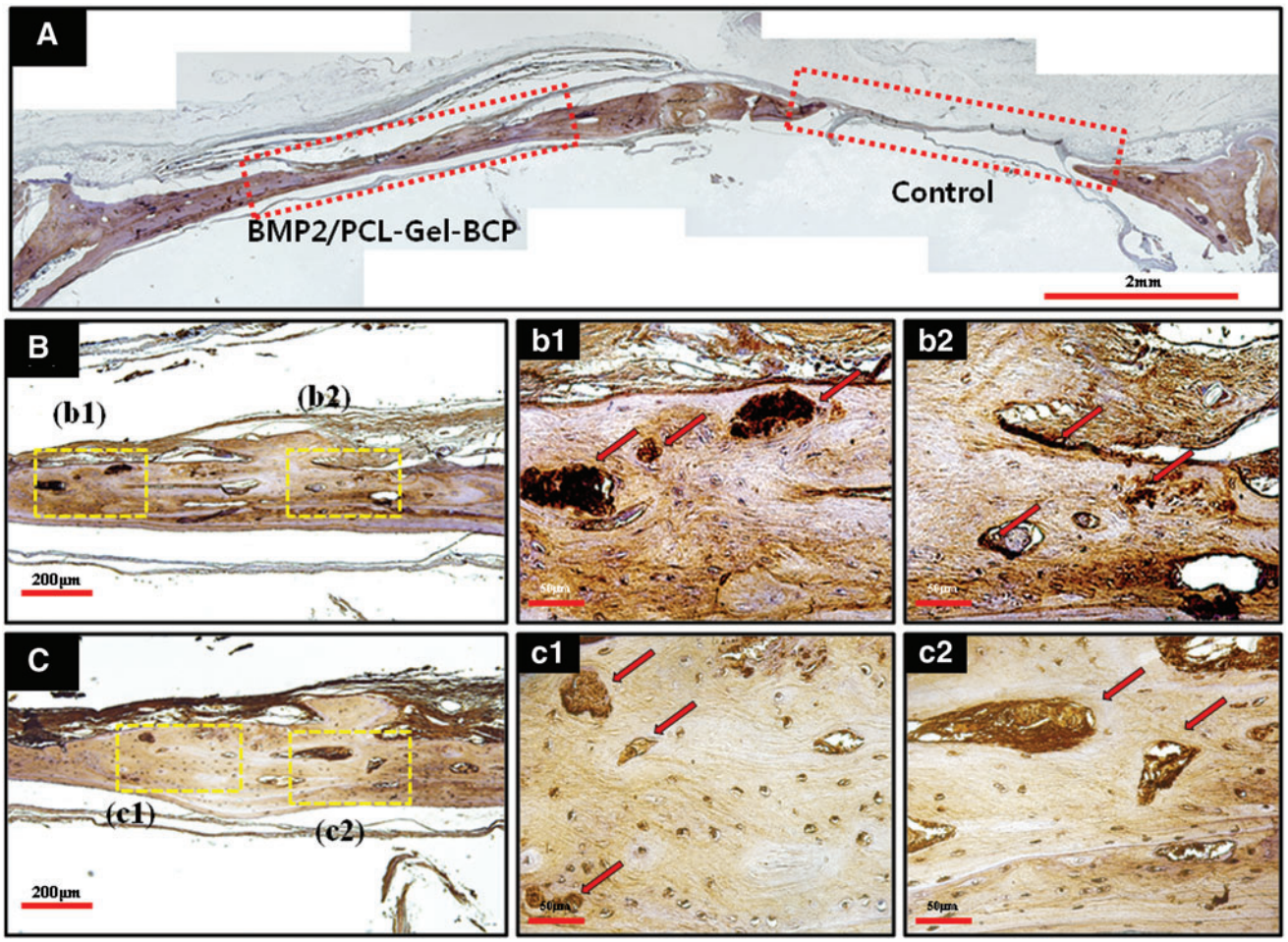

FIG. 8. **(A)** Representative immunohistochemical staining image of BMP-2/PCL–Gel–BCP (left) and control (right) labeled with OPN at 8 weeks. BMP-2/PCL–Gel–BCP implanted site detected with OPN **(B)** and OCN **(C)** was observed by higher magnification; **(b1, b2)** OPN, and **(c1, c2)** OCN. The red rectangles indicate defect zones; yellow rectangles indicate (b1, b2, c1, c2); red arrows indicate positive expressions of OPN and OCN. Color images available online at www.liebertpub.com/tea

a typical stained image labeled with OPN. Compared with the nonimplantation site (control), the BMP-2/PCL–Gel–BCP implanted group revealed positive expression as a brown color. Figure 8(B) and (C) are high magnification images of OPN and OCN detection, respectively. Expression of type I collagen, which is representative of initial proliferation and osteoblastic activity, was confirmed by M-T staining. OPN [Fig. 8(B)] and OCN [Fig. 8(C)] expression, which occurs at a later stage during ECM mineralization and bone formation, was observed as dark brown and is indicated by the arrows.

Discussion

BMP-2 has been widely applied to various scaffolds for bone tissue engineering, because of its excellent bone healing properties.[39–41] However, BMP-2 tends to disperse rather than act locally when incorporated into the human body. Therefore, BMP-2 must be compounded with a carrier to control its release over an extended time period.[30,41] Several kinds of polymer systems have been used as a carrier for BMP-2 to be stored and released.[30,42] In this study, BMP-2 was loaded on scaffolds using blend electrospinning so that growth factors could be mixed with the PCL–Gel polymer solution containing BCP particles, and the mixed solution was used directly in the electrospinning process. The matrix scaffold was a hybrid system containing ceramic/polymer and growth factors. The growth factors were located within the scaffold fibers rather than at the surface and the entire release profile was more sustained compared to that of physical adsorption. A sustained release-profile can be observed for more than several weeks using this method.

However, one of the problems when using blend electrospinning is a reduction in activity of the incorporated growth factors. They may lose bioactivity and stability because of structural changes in the organic solution condition.[43] Several strategies have been applied to prevent loss of bioactivity and to improve stability of the growth factors. Hydrophilic additives can be used as a strategy by minimizing the hydrophobic interactions between growth factors and the organic solvents.[43] Nie *et al.*[35] reported that using HAp particles as an additive can aid in the release of BMP-2 from fibers and also prevent deterioration due to hydrophilicity of the fibers. In our study, BCP nanoparticles were used not only to improve osteoconductivity, but also to stabilize BMP-2 bioactivity. BCP particles were loaded into the PCL–Gel blend and observed on the electrospun scaffolds by SEM and EDS (Fig. 1). XRD showed that the PCL–Gel–BCP scaffolds included peaks of both the BCP and PCL–Gel components. This observation indicates that the BCP particles were successfully delivered into the PCL–Gel scaffolds, and uniformly distributed inside the fibers. The presence of BMP-2 was shown by positive immunofluorescence staining [Fig. 2(A, B)]. BMP-2 release behavior and encapsulation efficiency were analyzed from the release profile. The release curve using a physical adsorption method shows a large burst release of growth factors during a narrow period at the very early stage of a few hours.[35,44] This release profile cannot be used for bone regeneration. Normally, release of growth factors from scaffolds is required for at least 30 days.[35] As shown in Figure 2(C), the initial release rate was high, but it decreased slowly after 5 days. This initial burst release may be related to growth factors located near the fiber surface, so the molecules diffused rapidly without degradation of the polymer. However, the remaining molecules within the fibers were released in a sustained manner because PCL has a slow degradation rate. After 31 days of release, 83.16% of the original amount of BMP-2 had been released. This high percentage indicates a high loading efficiency of growth factors with small amounts remaining for releasing during the late stage. This release behavior was suitable when considering bone remodeling time, which requires at least 30 days.

BMPs, which are members of the highly conserved transforming growth factor-β superfamily, play a critical role in tissue morphogenesis and bone formation. Among them, BMP-2 is one of the most potent osteoinductive signal proteins.[45–47] BMP-2 regulates various cellular functions such as growth, differentiation, secretion, and apoptosis.[45] In our study, BMP-2 was combined with the PCL–Gel–BCP scaffolds for delivery to a target site such as a large defect. The interaction between implanted materials and the cellular matrix is based on the binding of cell surface receptors with ligands, which promote specific cellular responses.[48] The *in vitro* studies illustrated in Figure 3 show that the MC3T3-E1 cells spread, attached, and proliferated very well on the BMP-2 scaffolds compared with those without BMP-2. Differences in cell behavior may have occurred due to the release of BMP-2. A total of $7.35\% \pm 1.28\%$ BMP-2 was released from the surface after 1 h, and the scaffold structure changed and affected cell adhesion and spreading because adhesion to the ECM is mediated by integrin binding with the material surface [Fig. 2(C)].[49] The presence of BMP-2 affected the interactions between cells and the scaffolds by binding to cell surface receptors. This binding may trigger biochemical reactions that change cell function and behavior and finally increase cell proliferation and differentiation.[21] ALP and OPN staining was used as a biochemical marker to determine the osteoblastic phenotype. The BMP-2-loaded scaffolds showed intense staining after 7 days compared with that of the PCL–Gel–BCP scaffolds. It also indicates BMP-2 release from the scaffolds influenced cell differentiation over time.

The Micro-CT and histological analyses revealed active bone regeneration on the BMP-2/PCL–Gel–BCP scaffolds. The BMP-2 released from the scaffolds enhanced bone regeneration. Osteoblasts migrated and proliferated from the interface with host bone to the center following scaffold implantation by promoting bone binding between the implanted material and the host bone tissue. Both the BMP-2/PCL–Gel–BCP and PCL–Gel–BCP scaffolds showed good osteogenesis and a large amount of newly formed bone containing viable osteocytes was observed compared with that in the control group. This result indicates that PCL–Gel–BCP scaffolds support bone formation sufficiently without BMP-2 loading and that they have good biocompatibility *in situ*. The efficiency of new bone formation was enhanced dramatically by delivering BMP-2, particularly at the initial stage. All of the results indicate that the BMP-2-loaded PCL–Gel–BCP scaffolds may biologically stimulate the surrounding cells to induce osteogenesis, and they retained the needed time for new bone formation and release during the long term by carrying the BMP-2 molecules to the defect sites. Finally, rapid and early bone regeneration occurred effectively. Bone-specific proteins such as OPN

and OCN are important factors for bone differentiation and mineralization.[50] In the immunocytochemical analysis, some nodules stained dark brown (indicated by arrows), where the BMP-2/PCL–Gel–BCP scaffolds were implanted. These were active osteoids, which are the organic portion of the bone matrix that forms before the maturation of bone tissue.[51] These nodules become mineralized bone tissue, and other parts that stained faint brown indicated that the bone tissue had already matured. New bone density was almost similar to native bone within 8 weeks postimplantation.[30] In particular, the BMP-2/PCL–Gel–BCP group revealed thick mineralized bone tissue.

Conclusion

A novel BMP-2/PCL–Gel–BCP fibrous scaffold hybrid system combining ceramic/polymers and growth factors was fabricated using an electrospinning process. BCP particles were distributed into the PCL–Gel blends and BMP-2 was loaded inside the fibers. The *in vitro* study showed that BMP-2 was released from the scaffolds with appropriately sustained release behavior, which positively influenced cell behavior and differentiation. The release of BMP-2 helped enhance bone formation at the early stage. Our results suggest that BMP-2/PCL–Gel–BCP electrospun scaffolds can be used for bone tissue regeneration and local delivery of biomolecules.

Acknowledgments

This article was supported by the Mid-career Research Program through NRF grant funded by the MEST (No. 2009-0092808), Republic of Korea and partially supported by Soonchunhyang University Research Fund. The authors would like to thank Mr. Shin-Woo Kim for the contributions of *in vivo* operation.

Disclosure Statement

No competing financial interests exist.

References

1. Naveena, N., Venugopal, J., Rajeswari, R., Sundarrajan, S., Sridhar, R., Shayanti, M., Narayanan, S., and Ramakrishna, S. Biomimetic composites and stem cells interaction for bone and cartilage tissue regeneration. J Mater Chem **22,** 5239, 2012.
2. Stevens, M.M. Biomaterials for bone tissue engineering. Mater Today **11,** 18, 2008.
3. Allo, B.A., Costa, D.O., Dixon, S.J., Mequanint, K., and Rizkalla, A.S. Bioactive and biodegradable nanocomposites and hybrid biomaterials for bone regeneration. J Funct Biomater **3,** 432, 2012.
4. Del Gaudio, C., Baiguera, S., Boieri, M., Mazzanti, B., Ribatti, D., Bianco, A., and Macchiarini, P. Induction of angiogenesis using VEGF releasing genipin-crosslinked electrospun gelatin mats. Biomaterials **34,** 7754, 2013.
5. Meinel, A.J., Germershaus, O., Luhmann, T., Merkle, H.P., and Meinel, L. Electrospun matrices for localized drug delivery: current technologies and selected biomedical applications. Eur J Pharm Biopharm **81,** 1, 2012.
6. Pant, H.R., Neupane, M.P., Pant, B., Panthi, G., Oh, H.-J., Lee, M.H., and Kim, H.Y. Fabrication of highly porous poly (ε-caprolactone) fibers for novel tissue scaffold via water-bath electrospinning. Colloids Surf B Biointerfaces **88,** 587, 2011.
7. Bhattarai, S.R., Bhattarai, N., Yi, H.K., Hwang, P.H., Cha, D.I., and Kim, H.Y. Novel biodegradable electrospun membrane: scaffold for tissue engineering. Biomaterials **25,** 2595, 2004.
8. Fu, S., Ni, P., Wang, B., Chu, B., Peng, J., Zheng, L., Zhao, X., Luo, F., Wei, Y., and Qian, Z. *In vivo* biocompatibility and osteogenesis of electrospun poly(ε-caprolactone)–poly(ethylene glycol)–poly(ε-caprolactone)/nano-hydroxyapatite composite scaffold. Biomaterials **33,** 8363, 2012.
9. Sill, T.J., and von Recum, H.A. Electrospinning: applications in drug delivery and tissue engineering. Biomaterials **29,** 1989, 2008.
10. Dash, T.K., and Konkimalla, V.B. Poly-ε-caprolactone based formulations for drug delivery and tissue engineering: a review. J Control Release **158,** 15, 2012.
11. Ji, W., Yang, F., Ma, J., Bouma, M.J., Boerman, O.C., Chen, Z., van den Beucken, J.J.J.P., and Jansen, J.A. Incorporation of stromal cell-derived factor-1α in PCL/gelatin electrospun membranes for guided bone regeneration. Biomaterials **34,** 735, 2013.
12. Oh, S.H., Park, I.K., Kim, J.M., and Lee, J.H. *In vitro* and *in vivo* characteristics of PCL scaffolds with pore size gradient fabricated by a centrifugation method. Biomaterials **28,** 1664, 2007.
13. Chong, E.J., Phan, T.T., Lim, I.J., Zhang, Y.Z., Bay, B.H., Ramakrishna, S., and Lim, C.T. Evaluation of electrospun PCL/gelatin nanofibrous scaffold for wound healing and layered dermal reconstitution. Acta Biomater **3,** 321, 2007.
14. Huang, Y., Onyeri, S., Siewe, M., Moshfeghian, A., and Madihally, S.V. *In vitro* characterization of chitosan–gelatin scaffolds for tissue engineering. Biomaterials **26,** 7616, 2005.
15. Kang, H.-W., Tabata, Y., and Ikada, Y. Fabrication of porous gelatin scaffolds for tissue engineering. Biomaterials **20,** 1339, 1999.
16. Vandelli, M.A., Rivasi, F., Guerra, P., Forni, F., and Arletti, R. Gelatin microspheres crosslinked with d,l-glyceraldehyde as a potential drug delivery system: preparation, characterisation, *in vitro* and *in vivo* studies. Int J Pharm **215,** 175, 2001.
17. Ba Linh, N.T., Min, Y.K., and Lee, B.-T. Hybrid hydroxyapatite nanoparticles-loaded PCL/GE blend fibers for bone tissue engineering. J Biomater Sci Polym Ed **24,** 520, 2012.
18. Gautam, S., Dinda, A.K., and Mishra, N.C. Fabrication and characterization of PCL/gelatin composite nanofibrous scaffold for tissue engineering applications by electrospinning method. Mater Sci Eng C Mater Biol Appl **33,** 1228, 2013.
19. Lee, J., Yoo, J.J., Atala, A., and Lee, S.J. The effect of controlled release of PDGF-BB from heparin-conjugated electrospun PCL/gelatin scaffolds on cellular bioactivity and infiltration. Biomaterials **33,** 6709, 2012.
20. Zhang, Y., Ouyang, H., Lim, C.T., Ramakrishna, S., and Huang, Z.-M. Electrospinning of gelatin fibers and gelatin/PCL composite fibrous scaffolds. J Biomed Mater Res B Appl Biomater **72B,** 156, 2005.
21. Zhang, H., Migneco, F., Lin, C.Y., and Hollister, S.J. Chemically-conjugated bone morphogenetic protein-2 on three-dimensional polycaprolactone scaffolds stimulates osteogenic activity in bone marrow stromal cells. Tissue Eng Part A **16,** 3441, 2010.
22. Li, C., Vepari, C., Jin, H.-J., Kim, H.J., and Kaplan, D.L. Electrospun silk-BMP-2 scaffolds for bone tissue engineering. Biomaterials **27,** 3115, 2006.

23. AbdulQader, S.T., Rahman, I.A., Ismail, H., Ponnuraj Kannan, T., and Mahmood, Z. A simple pathway in preparation of controlled porosity of biphasic calcium phosphate scaffold for dentin regeneration. Ceramics Int **39,** 2375, 2013.
24. Ramay, H.R.R., and Zhang, M. Biphasic calcium phosphate nanocomposite porous scaffolds for load-bearing bone tissue engineering. Biomaterials **25,** 5171, 2004.
25. Frohbergh, M.E., Katsman, A., Botta, G.P., Lazarovici, P., Schauer, C.L., Wegst, U.G.K., and Lelkes, P.I. Electrospun hydroxyapatite-containing chitosan nanofibers crosslinked with genipin for bone tissue engineering. Biomaterials **33,** 9167, 2012.
26. Lü, L.-X., Zhang, X.-F., Wang, Y.-Y., Ortiz, L., Mao, X., Jiang, Z.-L., Xiao, Z.-D., and Huang, N.-P. Effects of hydroxyapatite-containing composite nanofibers on osteogenesis of mesenchymal stem cells *in vitro* and bone regeneration *in vivo*. ACS Appl Mater Interfaces **5,** 319, 2012.
27. Rajzer, I., Menaszek, E., Kwiatkowski, R., and Chrzanowski, W. Bioactive nanocomposite PLDL/nano-hydroxyapatite electrospun membranes for bone tissue engineering. J Mater Sci Mater Med **25,** 1239, 2014.
28. Patel, Z.S., Young, S., Tabata, Y., Jansen, J.A., Wong, M.E.K., and Mikos, A.G. Dual delivery of an angiogenic and an osteogenic growth factor for bone regeneration in a critical size defect model. Bone **43,** 931, 2008.
29. Zhang, Z., Hu, J., and Ma, P.X. Nanofiber-based delivery of bioactive agents and stem cells to bone sites. Adv Drug Deliv Rev **64,** 1129, 2012.
30. Nguyen, T.-H., and Lee, B.-T. *In vitro* and *in vivo* studies of rhBMP2-coated PS/PCL fibrous scaffolds for bone regeneration. J Biomed Mater Res A **101A,** 797, 2013.
31. Niu, X., Feng, Q., Wang, M., Guo, X., and Zheng, Q. Porous nano-HA/collagen/PLLA scaffold containing chitosan microspheres for controlled delivery of synthetic peptide derived from BMP-2. J Control Release **134,** 111, 2009.
32. Chu, T.-M.G., Warden, S.J., Turner, C.H., and Stewart, R.L. Segmental bone regeneration using a load-bearing biodegradable carrier of bone morphogenetic protein-2. Biomaterials **28,** 459, 2007.
33. Yilgor, P., Hasirci, N., and Hasirci, V. Sequential BMP-2/BMP-7 delivery from polyester nanocapsules. J Biomed Mater Res A **93A,** 528, 2010.
34. Lee, B.-T., Youn, M.-H., Paul, R.K., Lee, K.-H., and Song, H.-Y. *In situ* synthesis of spherical BCP nanopowders by microwave assisted process. Mater Chem Phys **104,** 249, 2007.
35. Nie, H., Soh, B.W., Fu, Y.-C., and Wang, C.-H. Three-dimensional fibrous PLGA/HAp composite scaffold for BMP-2 delivery. Biotechnol Bioeng **99,** 223, 2008.
36. Petrie, C., Tholpady, S., Ogle, R., and Botchwey, E. Proliferative capacity and osteogenic potential of novel dura mater stem cells on poly-lactic-co-glycolic acid. J Biomed Mater Res A **85A,** 61, 2008.
37. Story, B.J., Wagner, W.R., Gaisser, D.M., Cook, S.D., and Rust-Dawicki, A.M. *In vivo* performance of a modified CSTi dental implant coating. Int J Oral Maxillofac Implants **13,** 749, 1998.
38. Nguyen, T.B., and Lee, B.T. A combination of biphasic calcium phosphate scaffold with hyaluronic acid-gelatin hydrogel as a new tool for bone regeneration. Tissue Eng Part A **20,** 1993, 2014.
39. Fu, Y.-C., Nie, H., Ho, M.-L., Wang, C.-K., and Wang, C.-H. Optimized bone regeneration based on sustained release from three-dimensional fibrous PLGA/HAp composite scaffolds loaded with BMP-2. Biotechnol Bioeng **99,** 996, 2008.
40. Park, K.-H., Kim, H., Moon, S., and Na, K. Bone morphogenic protein-2 (BMP-2) loaded nanoparticles mixed with human mesenchymal stem cell in fibrin hydrogel for bone tissue engineering. J Biosci Bioeng **108,** 530, 2009.
41. Takahashi, Y., Yamamoto, M., and Tabata, Y. Enhanced osteoinduction by controlled release of bone morphogenetic protein-2 from biodegradable sponge composed of gelatin and β-tricalcium phosphate. Biomaterials **26,** 4856, 2005.
42. Yokota, S., Sonohara, S., Yoshida, M., Murai, M., Shimokawa, S., Fujimoto, R., Fukushima, S., Kokubo, S., Nozaki, K., Takahashi, K., Uchida, T., Yokohama, S., and Sonobe, T. A new recombinant human bone morphogenetic protein-2 carrier for bone regeneration. Int J Pharm **223,** 69, 2001.
43. Ji, W., Sun, Y., Yang, F., Beucken, J.J.P., Fan, M., Chen, Z., and Jansen, J. Bioactive electrospun scaffolds delivering growth factors and genes for tissue engineering applications. Pharm Res **28,** 1259, 2011.
44. Lo, K.W.H., Ulery, B.D., Ashe, K.M., and Laurencin, C.T. Studies of bone morphogenetic protein-based surgical repair. Adv Drug Deliv Rev **64,** 1277, 2012.
45. Liu, H.-W., Chen, C.-H., Tsai, C.-L., and Hsiue, G.-H. Targeted delivery system for juxtacrine signaling growth factor based on rhBMP-2-mediated carrier-protein conjugation. Bone **39,** 825, 2006.
46. Schmitt, J.M., Hwang, K., Winn, S.R., and Hollinger, J.O. Bone morphogenetic proteins: An update on basic biology and clinical relevance. J Orthop Res **17,** 269, 1999.
47. Vo, T.N., Kasper, F.K., and Mikos, A.G. Strategies for controlled delivery of growth factors and cells for bone regeneration. Adv Drug Deliv Rev **64,** 1292, 2012.
48. Puleo, D.A., and Nanci, A. Understanding and controlling the bone–implant interface. Biomaterials **20,** 2311, 1999.
49. Schmitt, S.K., Murphy, W.L., and Gopalan, P. Crosslinked PEG mats for peptide immobilization and stem cell adhesion. J Mater Chem B **1,** 1349, 2013.
50. Wang, H., Li, Y., Zuo, Y., Li, J., Ma, S., and Cheng, L. Biocompatibility and osteogenesis of biomimetic nano-hydroxyapatite/polyamide composite scaffolds for bone tissue engineering. Biomaterials **28,** 3338, 2007.
51. Park, J.K., Shim, J.-H., Kang, K.S., Yeom, J., Jung, H.S., Kim, J.Y., Lee, K.H., Kim, T.-H., Kim, S.-Y., Cho, D.-W., and Hahn, S.K. Solid Free-Form Fabrication of tissue-engineering scaffolds with a poly(lactic-co-glycolic acid) grafted hyaluronic acid conjugate encapsulating an intact bone morphogenetic protein-2/poly(ethylene glycol) complex. Adv Funct Mater **21,** 2906, 2011.

Address correspondence to:
Byong-Taek Lee, PhD
Department of Regenerative Medicine
College of Medicine
Soonchunhyang University
366-1, Ssangyong Dong
Cheonan 330-090
Republic of Korea

E-mail: lbt@sch.ac.kr

Received: January 29, 2014
Accepted: May 28, 2014
Online Publication Date: September 30, 2014